Article ID: 1006-8775(2020) 01-0027-08

A STUDY ON THE PREDICT ABILITY OF GRAPES MODEL OVER SOUTH CHINA: COMPARISONS BY TWO INITIALIZATION CONDITIONS BETWEEN ECMWF AND NCEP

ZHONG Shui-xin (钟水新), CHEN Zi-tong (陈子通)
(Guangdong Provincial Key Laboratory of Regional Numerical Weather Prediction/ Institute of Tropical and Marine Meteorology, CMA, Guangzhou 510641 China)

Abstract: This paper aims to assess the performances of different model initialization conditions (ICs) and lateral boundary conditions between two global models (GMs), i. e., the European Centre for Medium-Range Weather Forecasts (ECMWF) and National Centers for Environmental Prediction (NCEP), on the accuracy of the Global / Regional Assimilation and Prediction System (GRAPES) forecasts for south China. A total of 3-month simulations during the rainy season were examined and a specific case of torrential rain over Guangdong Province was verified. Both ICs exhibited cold biases over south China, as well as a strong dry bias over the Pearl River Delta (PRD). In particular, the ICs from the ECMWF had a stronger cold bias over the PRD region and a more detailed structure than NCEP. In general, the NCEP provided a realistic surface temperature compared to the ECMWF over south China. Moreover, GRAPES initialized by the NCEP had better simulations of both location and intensity of precipitation than by the ECWMF. The results presented in this paper could be used as a general guideline to the operational numerical weather prediction that uses regional models driven by the GMs.

Key words: model initialization conditions; GRAPES; torrential rain; cold bias
CLC number: P467 **Document code:** A
https://doi.org/10.16555/j.1006-8775.2020.003

1 INTRODUCTION

With the development of numerical weather prediction (NWP) models and enhancement of computing ability, global forecast systems (GFS) provide more and more precise forecasts at a finer resolution. Besides, global models (GMs) provide the meso-scale models with initialization conditions (IC) and lateral boundary conditions (LBCs). Currently, two GFS models, i. e., the European Centre for Medium-Range Weather Forecasts (ECMWF) and National Centers for Environmental Prediction (NCEP), are comprehensively used as the IC in most operational NWP meso-scale models, e. g., the nonhydrostatic fifth-generation Pennsylvania State University-NCAR Mesoscale Model (MM5) model (Amengual et al.[1]), the Advanced Regional Prediction System (ARPS) (Xue et al.[2]), the Weather Research and Forecasting Model (WRF) (Skamarock et al.[3]) and the Global / Regional Assimilation and Prediction System (GRAPES) model (Chen et al. [4]; Zhong et al.[5-6]).

The inaccuracy of model dynamics, physics and errors generated by data assimilation methods could reduce the forecast abilities of these meso-scale models. Besides, errors in GFS models could also degrade the forecast skill of the NWP models, e. g., regional model which obtain IC and lateral boundary conditions (LBCs) from global model (Kumar et al.[7]). Therefore, it is necessary to evaluate the performances of GFS model on driving the operational meso-scale model. Newman et al. [8] compared the NCEP, NASA and ECMWF over the tropical west Pacific warm pool, and it was found that the ECMWF was the best among the three with observations in this region. Buizza et al. [9] summarized the methodologies used in the ECMWF, NCEP and the meteorological service of Canada (MSC) to conduct a 3-month simulation of the effect of IC uncertainties in ensemble forecasting. Duan et al. [10] evaluated the performances of ensemble prediction systems (EPSs) from the China Meteorological Administration (CMA), ECMWF, NCEP, and the Japan Meteorological Agency (JMA). Their results both indicated that the ECMWF ensemble forecast system had the best overall performances.

A few studies compared the performances of different IC from GFS models on the meso-scale NWP model forecasts. Amengual et al. [1] compared the performances of NCEP and ECMWF initialization on the simulation of a flash-flood episode by MM5 model.

Received 2019-05-23; **Revised** 2019-12-15; **Accepted** 2020-02-15
Foundation item: National Key R&D Program of China (2018YFC1506901); National Natural Science Foundation of China (41505084); Guangzhou Science and Technology Project (201804020038)
Biography: ZHONG Shui-xin, associate researcher, primarily undertaking research on weather diagnosis and numerical weather prediction.
Corresponding author: ZHONG Shui-xin, e-mail: zhongshui xin@126.com

Kumar et al. [7, 11] examined the impacts of ECMWF, NCEP and National Centre for Medium Range Weather Forecasting (NCMRWF) on the WRF model forecast over the Indian Region. Their results demonstrated that forecasts initialized from the ECMWF analysis were closer to Atmospheric Infrared Sounder (AIRS) retrieved profiles and in-situ observations compared to analysis from other global models. Zhong et al. [5] examined the performances of GRAPES on the simulations of the 20 July 2016 flash-flood episode over south China. The results showed that GRAPES failed to predict the extreme precipitation and had a systematic cold bias over the Guangdong and Guangxi (thereafter LG) regions.

The GFS model by NCEP forecasts are currently in use as IC for some of the regional NWP centers in CMA, e. g., the Shanghai Meteorological Center. The Guangzhou Regional Meteorological Center substituted the NCEP-GFS forecasts by ECMWF forecasts as the IC for GRAPES model since 2017. In this paper, the performances of these two GFS models on deriving the GRAPES model are evaluated, especially over the LG during the annually first rainy season. This study assesses the performances by using different ICs of ECMWF and NCEP on GRAPES simulations of surface temperature, wind, precipitation, and water vapor. Questions that motivate the study include the following:

(1) What are the limitations of using the NCEP and ECMWF as the ICs in the simulation for south China during the annually first rainy season?

(2) What are performances of the GRAPES model on the simulations over south China by using different IC and LBCs from NCEP and ECMWF forecasts?

(3) What are biases of GRAPES model on the simulation in the annually first rainy season? Are these biases from similar errors by the ICs?

The paper is organized as follows. Section 2 introduces details of the model setup and observational data used in this study. Section 3 examines the prediction skill of surface elements by different ICs of ECMWF and NCEP in a 3-month simulation. Section 4 evaluates the prediction and verification of a particular case in the LG regions during the annually first rainy season. Conclusions and discussions are given in section 5.

2 DATA AND MODEL

2.1 *Experimental design*

To assess GRAPES simulations over south China by using different ICs of ECMWF and NCEP, we evaluate the performances of these two GFS models on deriving the GRAPES model during the annually first rainy season. The GFS forecasts of ECMWF with horizontal resolution of 0.1° × 0.1° are obtained for the meso-scale model initialization. The vertical layer consists of 17 vertical pressure levels in the ECMWF model analysis. The GFS forecasts of NCEP are used in this study with horizontal resolution of 0.5° × 0.5° at the same vertical pressure layers and forecast intervals. The initial time of the experiment is 1200 UTC from April to June 2018, and the analyses data of GMs refers to the original data at initial time in this study.

The observations obtained in this study are the hourly automatic meteorological observations from April to June 2018 over south China. The surface meteorological variables include surface temperature, winds, relative humidity, surface pressure and precipitation amount at 1-h intervals. The specific humidity in this study is calculated by using the hourly surface observation at each station

$$Qv = C_r \cdot rh \cdot \frac{es}{P_s - 0.378 * es} \quad (1)$$

where C_r is a constant $(6.22 \cdot 10^{-3})$, P_s, rh and es represent surface pressure, relative humidity and saturated vapor pressure, respectively.

2.2 *GRAPES model*

The model used in this study is an operational model over south China based on GRAPES. The simulation domain comprises 913 × 513 grid points with horizontal resolution of 0.03° × 0.03°, and 65 layers in the vertical direction. The model consists of serval separated model physic process including planetary boundary layer (PBL) parameterization schemes (Hong and Pan [12]; Hong and Dudhia [13]), gravity wave drag induced by sub-grid orography (GWDO, Zhong and Chen [14]), sub-grid orographic parameterization scheme (Zhong et al.[6]), a simplified land surface model based on SLAB (SMS), the Rapid Radiative Transfer Model (RRTM, Verlinden and Szoeke [15]) and the Rapid Radiative Transfer Model for global climate models (RRTMG, Mukkavilli [16]).

3 MONTHLY VERIFICATIONS

3.1 *Verifications of GFS analysis*

In this section, both the ICs from GFS data of ECMWF and NCEP are verified by using a 3-month observation and a day-by-day simulation from April to June 2018. Fig. 1 shows the mean surface temperature and specific humidity by ECMWF and NCEP and observations over south China. It can be seen that the surface temperature of both GMs show a decreasing trend from the South China Sea (SCS) to the inland, and both GMs data capture a relative warm background in the LG regions than in other areas. The ECMWF provides a more detailed representation of surface temperature than NCEP. For example, it captures the low temperature over the mountainous regions, e.g., the Lian Hua Mountains (LHMs) and the Yun Kai Mountains (YKMs) in Guangdong Province. However, the initialization from NCEP has a warmer environment than that from the ECMWF in the coastal areas. In particular, the surface temperature is much higher than that by the ECMWF over the Pearl River Delta (PRD).

The overall temperature over the PRD is higher than 25 degree by NCEP, while the ECMWF shows a lower temperature over this region. Moreover, the surface temperature from the GMs of NCEP is also higher than that from the GMs of ECMWF over south Guangxi (GX) Region.

It also can be seen that the specific humidity of both GMs data shows a similar characteristic over south China, and its distribution is consistent with the surface temperature and local topographic characteristics. For example, the high specific humidity is consistent with the low temperature, especially over the mountainous regions. Both ICs show a decreasing trend from the SCS to the inland with three lower water vapor centers over Jiangxi (JX) and Hunan (HN) Provinces and the PRD regions. However, the NCEP initialization provides a dryer environment than ECMWF does over south China, especially over the PRD regions. The general surface specific humidity over the LG is about 15 g kg^{-1} by NCEP, while that by the ECMWF reaches about 16-17 g kg^{-1} over this region. The ECMWF shows an overestimation of the water vapor over south China, while the NCEP presents a more consistent distributions of the water vapor over south China. Both ICs underestimate the high coverage of water vapor over the PRD regions. The observations show a high water vapor center over this region, while the ICs present an opposite low water vapor center over the PRD.

Note that warm and wet background is favorable for the formation of precipitation, which may cause extreme precipitation over this region, e.g., the extreme precipitation over Zengcheng district of Guangzhou on 7 May 2017. The 3-h accumulated rainfall in Xintang Town of Zengcheng reaches 382.6 mm, breaking the historical maximum of 3-h accumulated rainfall in Guangdong Province. However, none of the NWP models could predict this extreme precipitation, and both the GFS models show an underestimation of the surface temperature at about 3-4 degree over this region. As shown in Fig. 2, the surface temperature given by both ICs of NCEP and ECMWF generally show extreme cold biases over south China, especially over the PRD region. It reaches more than 30℃ in observations whereas it is less than 23℃ in the ICs. The vertical profile of temperature by both GMs, however, exhibits no significant bias in Hong Kong (Fig. 3), which is located over the south of the PRD regions.

Surface specific humidity over the PRD regions exhibits a low value center with less than 14 g kg^{-1} by both GMs, while the observations show an opposite distribution which reaches more than 20 g kg^{-1} in the high value center. The dry biases by the GMs could also be seen from the vertical profile at Hong Kong stations (Fig. 3), which the dry biases both reach about 1.2 g kg^{-1} at 850 hPa and 1.7 g kg^{-1} at 1000 hPa, respectively.

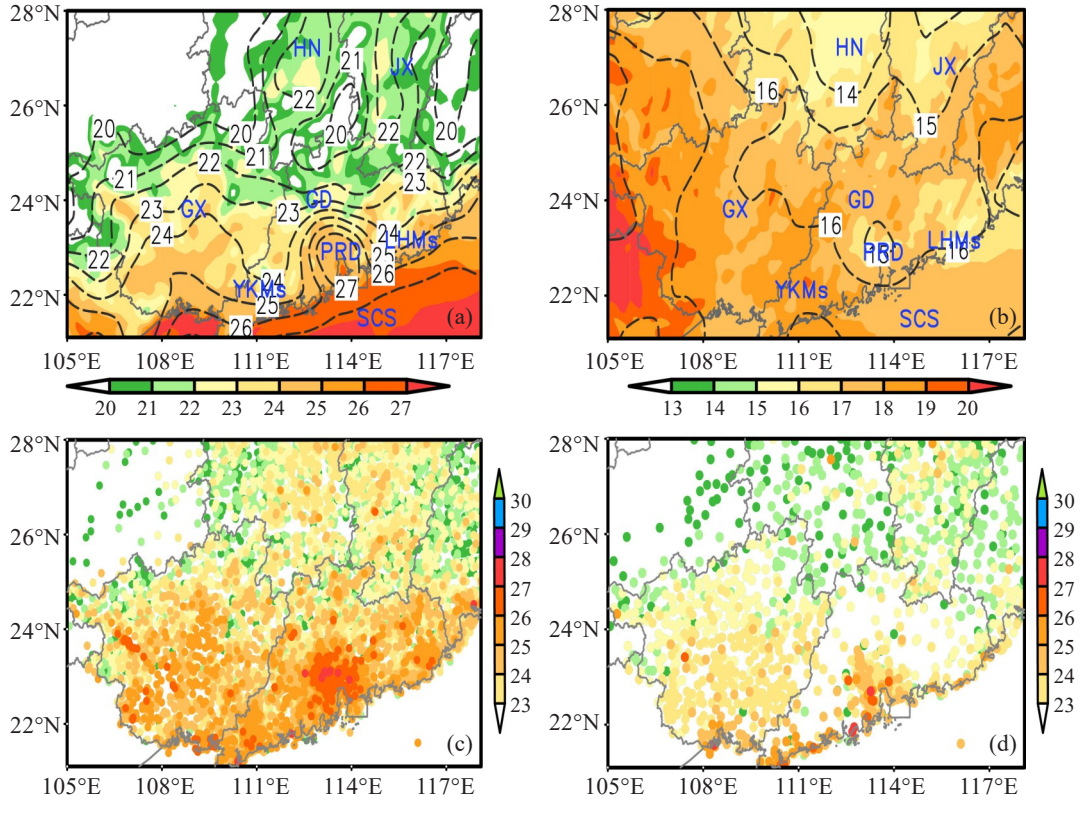

Figure 1. (a, c) Mean surface temperature (units: °C) and (b, d) surface specific humidity (units: g kg^{-1}). The shaded and dashed line in (a) and (b) denote initial conditions from ECMWF and NCEP, respectively. The color dots represent surface observations.

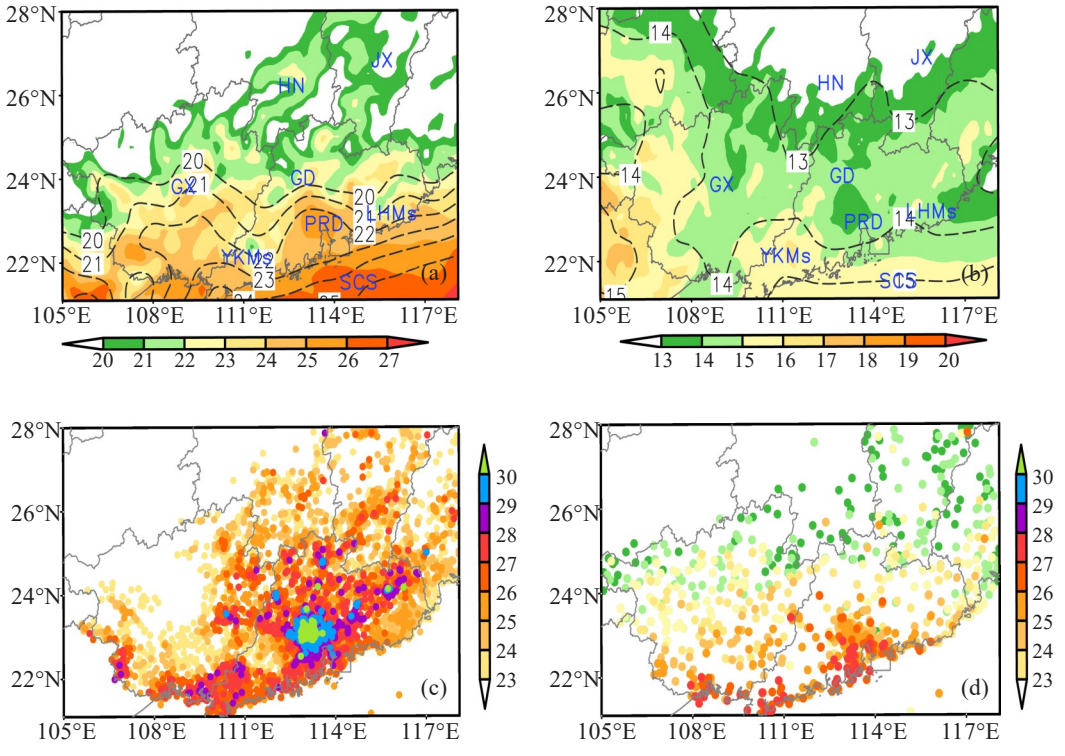

Figure 2. The same as Fig.1, but for 1200 UTC 7 May 2017.

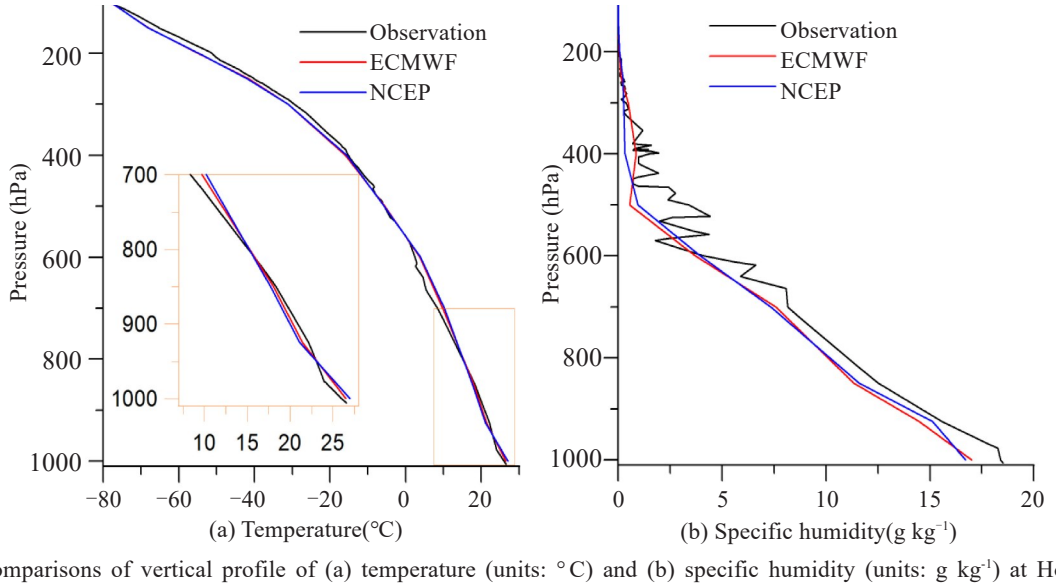

Figure 3. Comparisons of vertical profile of (a) temperature (units: °C) and (b) specific humidity (units: g kg^{-1}) at Hong Kong between observation (black line) and the initial conditions from ECMWF (red line) and NCEP (blue line).

3.2 *Comparisons of the simulations by GRAPES model*

In this section, the sensitive experiments of GRAPES initialized by ECMWF (GRAPES_EC) and NCEP (GRAPES_NC) are conducted to further discuss the impacts of the ICs and LBCs from GMs on operational NWP forecasts. The experiments are initialized at 1200 UTC for day-by-day simulations from April to June 2018. Fig. 4 gives the comparisons of the 24-h simulation of surface temperature and specific humidity between two experiments. Simulations of both experiments are approximately consistent with observations (Fig. 1). In particular, GRAPES_EC has a warmer forecast of surface temperature than GRAPES_NC, which is about 1℃ difference over most of areas in south China between the two experiments. Besides, the simulations show that GRAPES_NC has less specific humidity than GRAPES_EC does. Both simulations show a more consistent distribution of surface temperature and humidity with observations than the initializations by ECMWF and NCEP.

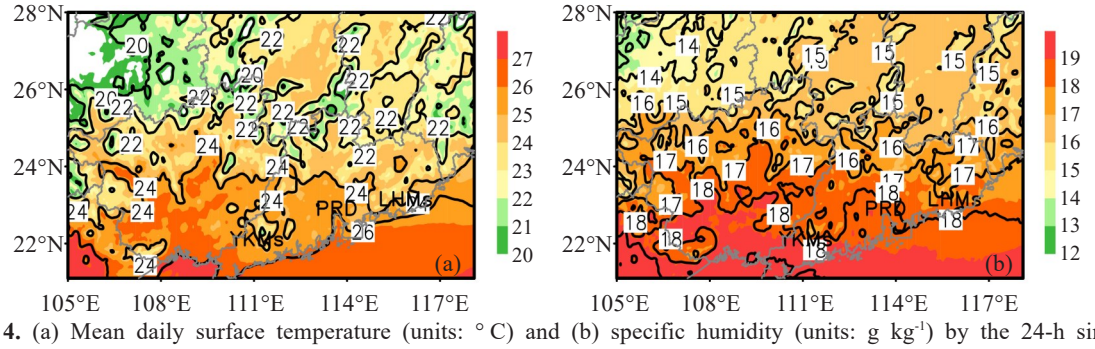

Figure 4. (a) Mean daily surface temperature (units: ° C) and (b) specific humidity (units: g kg^{-1}) by the 24-h simulation of GRAPES_EC (shaded) and GRAPES_NC (contour).

Figure 5 gives the simulations of 24-h accumulated precipitation by GRAPES_EC and GRAPES_NC. GRAPES generally captures the precipitation over south China. However, GRAPES_NC exhibits more consistent simulations with the observations than GRAPES_EC. For example, the simulations by GRAPES_NC has a better forecast accuracy in terms of the intensity and location of the precipitation compared to the observation, especially the strong rainfall center over the PRD region. The simulations of GRAPES_EC, however, are too far north over the coastal regions of Guangdong Province, and also overestimate the precipitation over the north of GX region. It should be noted that GRAPES has missed the strong precipitation over the LHMs and south coastal areas of GX region in both experiments, as it is often caused by local orographic effects and NWP model often fail to represent it realistically.

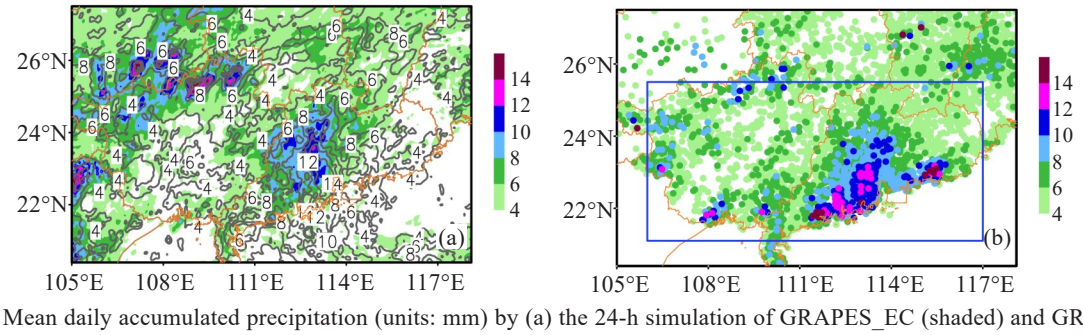

Figure 5. Mean daily accumulated precipitation (units: mm) by (a) the 24-h simulation of GRAPES_EC (shaded) and GRAPES_NC (contour) and (b) observations. The blue rectangle denotes the verification areas.

3.3 *Hourly verifications of GRAPES model with surface observations*

To further examine the impacts of the initializations from the GMs, we conducted hourly verifications of the simulation of GRAPES initialized by the ICs from ECMWF and NCEP with surface observations. The verification areas are mainly comprised of Guangdong and Guangxi regions. Verifications are conducted by calculating the root-mean-square error (RMSE) and bias between forecasts and observations, and the mathematical calculation equations are as follows:

$$\mathrm{RMSE} = \left[\frac{1}{N}\sum (F_C - O_B)^2\right]^{\frac{1}{2}} \quad (2)$$

$$\mathrm{OV}_{bias} = \frac{1}{N}\sum (F_C - O_B), \ (F_C > O_B) \quad (3)$$

$$\mathrm{UN}_{bias} = \frac{1}{N}\sum (F_C - O_B), \ (F_C < O_B) \quad (4)$$

where F_C is forecast, O_B is the observation and N is the number of stations in the verification region. OV_{bias} and UN_{bias} are the average biases by overestimation and underestimation, respectively.

Figure 6 shows the comparisons of 3-month averaged surface temperature between observations and simulation, as well as the comparisons of the average RMSE and bias between GRAPES_EC and GRAPES_NC. In general, GRAPES model can predict the diurnal variations of the surface temperature. It generally underestimate the surface temperature over south China. Both experiments exhibit the largest surface-temperature underestimation in the initialization, which are gradually alleviated within 12-h simulation, accompanying with an increasing RMSE by 12-h to 18-h simulation from morning to the noon growth by both experiments. Besides, GRAPS_NC shows smaller biases of surface temperature than GRAPES_EC does. Both experiments show significant reduction of stations by underestimation and overestimation of surface temperature after 12-h simulation, which might be caused by solar heating in the morning.

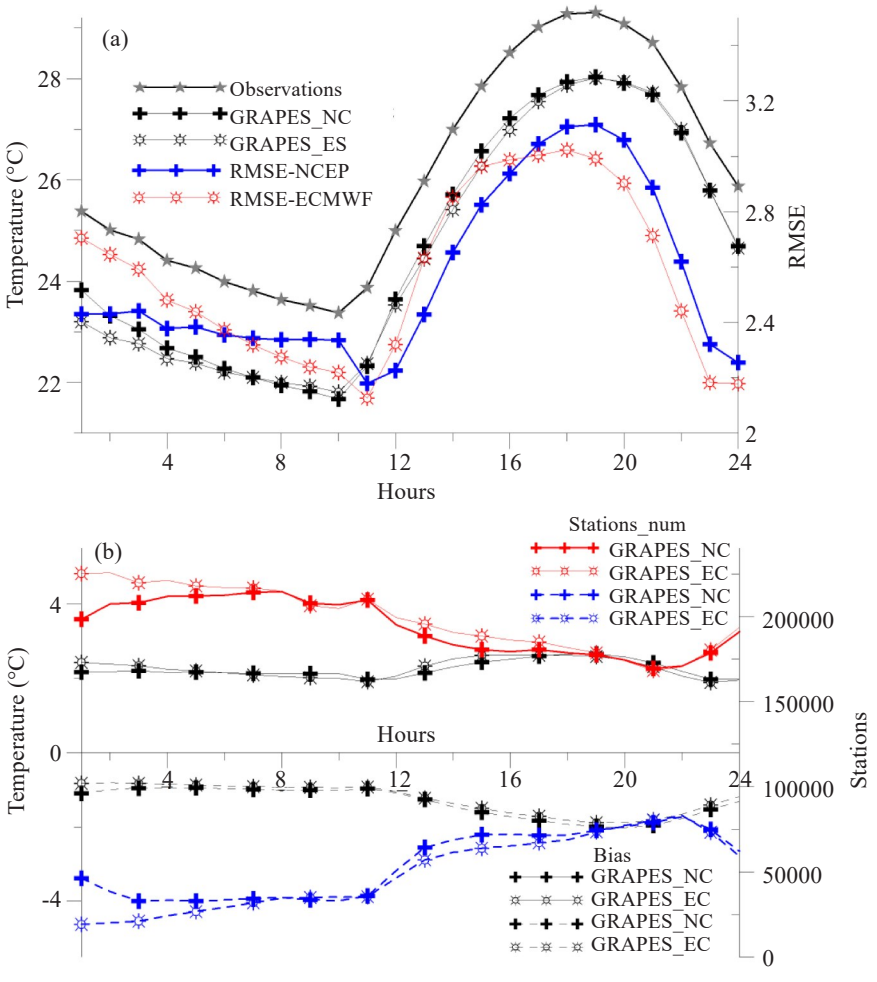

Figure 6. (a) Comparisons of hourly RMSE and mean surface temperature between observations and simulations by GRAPES_EC and GRAPES_NC. (b) Comparisons of hourly biases between OV_{bias} and UN_{bias}(black lines), and summation of the stations by overestimation (blue dotted line) (red solid line).

4 ILLUSTRATION OF TWO ICS DATA FOR THE TORRENTIAL RAINS STUDY

This section illustrates the south China precipitation case study initialized at 1200 UTC 18 April 2019 to examine performances of the IC and LBCs by different GMs on GRAPES simulation. The experiments are initialized by the two GMs as shown in the seasonal verification. Shown in Fig. 7 are the differences of surface temperature, surface specific humidity and surface water vapor flux between the initialization of the NCEP and ECMWF. It can be seen that the NCEP has a warmer surface temperature over most of south China, especially over the PRD region and east of Guangdong. Note also that the NCEP has more surface specific humidity over these regions than the ECMWF. Therefore, the NCEP provides a warmer and wetter background over south China than the ECMWF does.

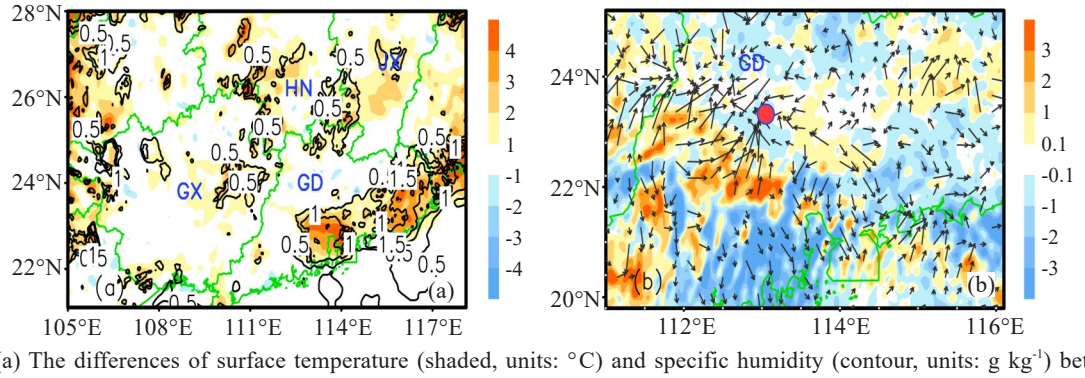

Figure 7. (a) The differences of surface temperature (shaded, units: °C) and specific humidity (contour, units: g kg^{-1}) between the initializations of NCEP and ECMWF; (b) 3-h average differences of surface winds and water vapor flux before the occurrence of the torrential rain (shaded, units: 10^5g m^{-1} s^{-1}). The red dot denotes the sounding location of Qing Yuan.

The differences of surface winds and water vapor flux confirm the stronger moisture convergence by GRAPES_NC (Fig. 7b), which provides a favorable environment for the convections. The 12-h simulation of sounding of Qing Yuan also shows that GRAPES_NC provides a more humid environment under 600 hPa than GRAPES_EC does, which exhibits a stronger dry bias especially at 850 hPa (Fig. 8).

Shown in Fig. 9 are the comparisons of simulation and observation of the 24-h accumulated precipitation over south China. GRAPES could predict the strong precipitation over the middle of Guangdong. However, GRAPES_NC provides a more realistic simulation of the precipitation location, whereas the simulation of precipitation location by GRAPES_EC is too north. The verifications show that GRAPES could predict the diurnal variations of the surface temperature (not shown), while both GRAPES_NC and GRAPES_EC underestimate the surface temperature during the nighttime and early morning. Furthermore, GRAPES_NC provides a better simulation of the surface temperature than GRAPES_EC.

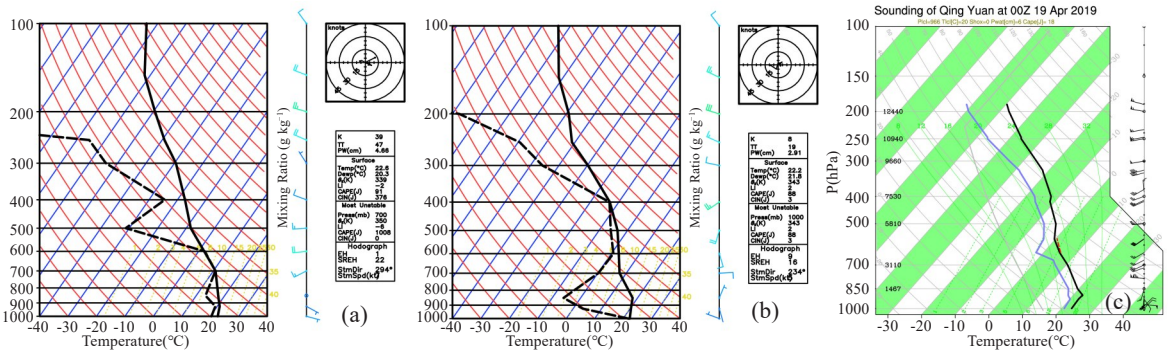

Figure 8. 12-h simulation of sounding of Qing Yuan by (a) GRAPES_NC and (b) GRAPES_EC and (c) observation.

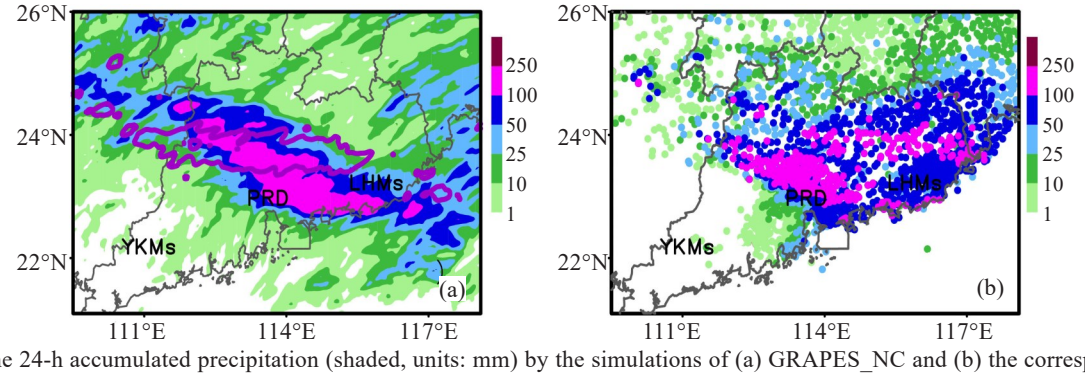

Figure 9. The 24-h accumulated precipitation (shaded, units: mm) by the simulations of (a) GRAPES_NC and (b) the corresponding observations at 1200 UTC 19 April 2019 over south China. The purple lines in (a) denotes the simulated precipitation by GRAEPS_EC (>100 mm).

5 DISCUSSION AND CONCLUSION

The main goal of this study is the assessment of the performances of different model initialization conditions and lateral boundary conditions between the global models of ECMWF and NCEP on the accuracy of the GRAPES forecasts over south China. A total of 3-month simulations during the flood season are examined and a specific case of torrential rain over Guangdong Province is verified. The results presented in this paper could be used as a general guideline for building operational NWP models which are driven by global models. Such a guideline could be helpful for the setup of operational NWP systems especially for the flood forecasting over south China.

The primary conclusion is that the ICs from NCEP provided a realistic surface temperature compared to the ECMWF during the warm season over south China. GRAPES shows more realistic simulations of both location and intensity of precipitation over Guangdong Province by using NCEP for initialization. Rather, the higher-resolution ECMWF provides a more detailed structure of the ICs than NCEP, while the ECMWF exhibits typical cold biases during the warm season over south China (Zhong et al.[5]). The straightforward difference of the surface temperature between the ICs of ECMWF and NCEP indicates that the biases in the initialization may lead to poor simulation of the strong precipitation over the Pearl River Delta (PRD) region. Besides, the dry biases in both GMs may also lead to the failures of the precipitation forecasts over the PRD region.

In general, the ICs from the GMs play an important role in the weather forecasts of meso-scale model over south China. Model techniques such as data assimilation (Buizza et al.[9]; Xiao et al.[17]; Zhang et al.[18]; Jang and Hong[19]) and initialization skills (Rakesh et al.[20]; Kumar et al.[7]; Yang et al.[21]; Chen et al.[22]) could be

used to alleviate these biases in the operational NWP models. On the other hand, the GRAPES model provides reliable weather forecasts over south China, and the verifications of ICs from GMs should be further examined. Future work on the initialization techniques for NWP models should be further developed to better represent the initialization conditions comparing to the observations.

Acknowledgments: The global model analyzed data provided by ECMWF and NCEP are acknowledged with sincere thanks.

REFERENCES:

[1] AMENGUAL A, ROMERO R, GÓMEZ M, et al. A hydrometeorological modeling study of a flash-flood event over Catalonia, Spain [J]. J Hydro, 2007, 8(3): 282-303, https://doi.org/10.1175/JHM577.1.

[2] XUE M, DROEGEMEIER K K, WONG V. The Advanced Regional Prediction System (ARPS) – A multi-scale nonhydrostatic atmospheric simulation and prediction model, Part I: Model dynamics and verification [J]. Meteorol Atmos Phys, 2000, 75(3-4): 161-193, https://doi.org/10.1007/s007030070003.

[3] SKAMAROCK W C, KLEMP J B, DUDHIA J, et al. A description of the advanced research WRF version 3, NCAR Technical Note [R]. Boulder: National Center for Atmospheric Research, 2008.

[4] CHEN D, XUE J, YANG X, et al. New generation of multi-scale NWP system (GRAPES): general scientific design [J]. Chin Sci Bull, 2008, 53(22): 3433-3445, http://doi.org/10.1007/s11434-008-0494-z.

[5] ZHONG S X, YANG S, GUO C Y, et al. Capabilities and limitations of GRAPES simulations of extreme precipitation in the warm sector over a complex orography [J]. J Trop Meteor, 2019, 25(2): 180-191, https://doi.org/10.16555/j.1006-8775.2019.02.005.

[6] ZHONG S X, CHEN Z T, XU D S, et al. Evaluating and improving wind forecasts over South China: The role of orographic parameterization in the GRAPES model [J]. Adv Atmos Sci, 2018, 35(6): 713-722, https://doi.org/10.1007/s00376-017-7157-4.

[7] KUMAR P, KISHTAWAL C M, PAL P K. Impact of ECMWF, NCEP, and NCMRWF global model analysis on the WRF model forecast over Indian Region [J]. Theor Appl Climatol, 2017, 127(1-2): 143-151, https://doi.org/10.1007/s00704-015-1629-1.

[8] NEWMAN M, SARDESHMUKH P D, BERGMAN J W. An assessment of the NCEP, NASA, and ECMWF reanalyses over the tropical west Pacific warm pool [J]. Bull Amer Meteor Soc, 2000, 81(1): 41-48, https://doi.org/10.1175/1520-0477(2000)081<0041:AAOTNN>2.3.CO;2

[9] BUIZZA R, HOUTEKAMER P L, PELLERIN G, et al. A comparison of the ECMWF, MSC, and NCEP global ensemble prediction systems [J]. Mon Wea Rev, 2005, 133 (5): 1076-1097, https://doi.org/10.1175/MWR2905.1.

[10] DUAN M, MA J, WANG P. Preliminary comparison of the CMA, ECMWF, NCEP, and JMA ensemble prediction systems [J]. Acta Meteor Sinica, 2012, 26(1): 26-40, https://doi.org/10.1007/s13351-012-0103-6.

[11] KUMAR P, KISHTAWAL C M, PAL P K. Skill of regional and global model forecast over Indian region [J]. Theor Appl Climatol, 2016, 123(3-4): 629-636, https://doi.org/ 10.1007/s00704-014-1361-2.

[12] HONG S Y, PAN H L. Nonlocal boundary layer vertical diffusion in a medium-range forecast model [J]. Mon Wea Rev, 1996, 124(10): 2322-2339, https://doi.org/10.1175/1520-0493(1996)124<2322:NBLVDI>2.0.CO;2.

[13] HONG S Y, NOH Y, DUDHIA J. A new vertical diffusion package with an explicit treatment of entrainment processes [J]. Mon Wea Rev, 2006, 134(9): 2318-2341, https://doi.org/10.1175/MWR3199.1.

[14] ZHONG S X, CHEN Z T. Improved wind and precipitation forecasts over South China using a modified orographic drag parameterization scheme [J]. J Meteor Res, 2015, 29(1): 132-143, https://doi. org / 10.1007 / s13351-014-4934-1.

[15] VERLINDEN K L, de SZOEKE S P. Simulating radiative fluxes through southeastern Pacific stratocumulus clouds during VOCALS-Rex[J]. J Atmos Oceanic Tech, 2018, 35 (4):821-836, https://doi.org/10.1175/JTECH-D-17-0169.1.

[16] MUKKAVILLI S K, PRASAD A A, TAYLOR R A, et al. Mesoscale simulations of Australian direct normal irradiance, featuring an extreme dust event [J]. J Appl Meteor, 2018, 57(3): 493-515, https://doi. org / 10.1175 / JAMC-D-17-0091.1.

[17] XIAO Q, SUN J. Multiple-radar data assimilation and short-range quantitative precipitation forecasting of a squall line observed during IHOP_2002 [J]. Mon Wea Rev, 2007, 135(10): 3381-3404, https://doi.org/10.1175/MWR3471.1.

[18] ZHANG F, ZHANG M, HANSEN J A. Coupling ensemble Kalman filter with four-dimensional variational data assimilation [J]. Adv Atmos Sci, 2009, 26(1): 1-8, https://doi.org/10.1007/s00376-009-0001-8.

[19] JANG J, HONG S Y. Quantitative forecast experiment of a heavy rainfall event over Korea in a global model: Horizontal resolution versus lead time issues[J]. Meteorol Atmos Phys, 2014, 124(3-4): 113-127, https://doi.org/10.1007/s00703-014-0312-x.

[20] RAKESH V, SINGH R, PAL P K, et al. Impacts of satellite-observed winds and total precipitable water on WRF short-range forecasts over the Indian Region during the 2006 summer monsoon[J]. Wea Forecasting, 2009, 24(6): 1706-1731, https://doi.org/10.1175/2009WAF2222242.1.

[21] YANG Mei-jin, GONG Jian-dong, WANG Rui-chun, et al. A comparison of the blending and constraining methods to introduce large-scale information into GRAPES mesoscale analysis [J]. J Trop Meteor, 2019, 25(2): 227-244, https://doi.org/10.16555/j.1006-8775.2019.02.009.

[22] CHEN J H, LIN S J, MAGNUSSON L, et al. Advancements in hurricane prediction with NOAA's next-generation forecast system [J]. Geophys Res Lett, 2019, 46(8): 4495-4501, https://doi. org / 10.1029 / 2019GL082410.

Citation: ZHONG Shui-xin and CHEN Zi-tong. A study on the predict ability of GRAPES model over south China: comparisons by two initialization conditions between ECMWF and NCEP [J]. J Trop Meteor, 26(1): 27-34, http://doi. org / 10.16555 / j. 1006-8775.2020.003.